Journal of Dynamics, Monitoring and Diagnostics, 2025, 4, 11-21
https://doi.org/10.37965/jdmd.2024.547

ISTP
RESEARCH ARTICLE

Class-Imbalanced Machinery Fault Diagnosis using Heterogeneous Data Fusion Support Tensor Machine

Zhishan Min,[1,2] Minghui Shao,[2] Haidong Shao,[2] and Bin Liu[3]
[1]Henan Pingzhi High-Voltage Switchgear Co., Ltd., Pingdingshan, China
[2]College of Mechanical and Vehicle Engineering, Hunan University, Changsha, China
[3]Department of Management Science, University of Strathclyde, Glasgow, UK

(Received 25 April 2024; Revised 04 June 2024; Accepted 09 December 2024; Published online 09 December 2024)

Abstract: The monitoring signals of bearings from single-source sensor often contain limited information for characterizing various working condition, which may lead to instability and uncertainty of the class-imbalanced intelligent fault diagnosis. On the other hand, the vectorization of multi-source sensor signals may not only generate high-dimensional vectors, leading to increasing computational complexity and overfitting problems, but also lose the structural information and the coupling information. This paper proposes a new method for class-imbalanced fault diagnosis of bearing using support tensor machine (STM) driven by heterogeneous data fusion. The collected sound and vibration signals of bearings are successively decomposed into multiple frequency band components to extract various time-domain and frequency-domain statistical parameters. A third-order heterogeneous feature tensor is designed based on multisensors, frequency band components, and statistical parameters. STM-based intelligent model is constructed to preserve the structural information of the third-order heterogeneous feature tensor for bearing fault diagnosis. A series of comparative experiments verify the advantages of the proposed method.

Keywords: class-imbalanced fault diagnosis; feature tensor; heterogeneous data fusion; support tensor machine

I. INTRODUCTION

With the development and progress of intelligent manufacturing, the requirements for the long-term safe operation of machinery equipment are becoming higher and higher. Rolling bearings are widely used in modern machinery equipment; however, due to their harsh working environment, they are prone to fatigue damage, which reduces the reliability of the equipment and may lead to accidents [1–3]. Therefore, an increasing number of scholars at home and abroad have conducted researches on rolling bearing fault diagnosis.

As a hot research topic of machine learning, deep learning methods have developed rapidly in recent years and have also been applied to the fault diagnosis of industrial equipment, such as deep belief network [4,5], recurrent neural network [6,7], and convolutional neural network (CNN) [8,9]. When these methods are applied to the fault diagnosis of rotating machinery, a large number of labeled training samples are often required [10]. However, in practical engineering applications, it is difficult to obtain enough fault samples of rotating machinery under different working conditions, that is, there exists class-imbalanced phenomenon between the fault samples and the normal samples [11]. In recent years, researchers have conducted a large amount of research on the issue of class-imbalanced fault diagnosis and have proposed numerous methods. Dablain *et al.* [12] developed a new data-level solution based on deep synthesized minority over-sampling technique that can process the original samples and generate high-quality assisted samples to balance the training set. Li *et al.* [13] proposed an auxiliary classier Wasserstein generative adversarial network with gradient penalty, which could stably generate high-quality samples of minority classes using the imbalanced training set. Cost-sensitive learning, as algorithm-level solution, can provide new perspective to address the class-imbalanced fault diagnosis problem [14]. He *et al.* [15] constructed a spatio-temporal graph neural network as the base model to achieve wind turbine fault detection, and the focus loss was used as the loss function in the training stage, which avoided the lack of attention to small samples in the traditional cross-entropy loss. Han *et al.* [16] designed a new cost matrix by adjusting the coefficient of the focal loss and then used the enhanced CNN to explore the representative features of fault samples. Ruan *et al.* [17] optimized one CNN and one GAN with two networks to provide a more balanced data set and to make corrections in the loss function of the neural network generator. The experimental results show that the bearing fault samples generated by optimized GAN contain more fault information than those generated by ordinary GAN. After data enhancement of unbalanced training set, the accuracy of CNN in fault classification can be significantly improved.

To a certain extent, the above research to some extent solves the problem that traditional deep learning models tend to shift their decision boundaries towards large sample data when the number of faulty samples is less than that of healthy samples during training. However, traditional deep learning models always require long training time and a large number of parameters, such as network topology, initial weights, biases, and other hyperparameters. Moreover, it is difficult to observe the learning process of neural network and their output results are hard to interpret. Support tensor machine (STM), an alternative of neural

Corresponding author: Haidong Shao (e-mail: hdshao@hnu.edu.cn).

© The Author(s) 2025. This is an open access article published under the CC BY license (https://creativecommons.org/licenses/by/4.0/).

network, holds the potential to solve all the above limitations that existed in the deep neural networks [18]. Wang *et al.* [19] proposed a new method for fault detection and multiple classification in rotating machinery based on kernel support tensor machine and multilinear principal component analysis. The performance and feasibility were evaluated by cases of bearing and gear. Yang *et al.* [20] proposed a bearing health monitoring framework based on multi-scale permutation entropy and pinball loss-based fuzzy STM. This framework could address the issue of losing important fault information when constructing tensor data through time-frequency image cropping and also hold anti-noise capability and low classification error. However, the above-mentioned researches based on STM are mostly based on single-source sensor signals, which may lead to instability and uncertainty of the intelligent diagnosis decision-making [21]. As rotating machinery equipment tends to be system integration, the coupling degree between various components is becoming higher and higher, leading to the monitoring signal from a single-source sensor not containing comprehensive information to effectively characterize the operation status [22].

This paper studies a new method for class-imbalanced fault diagnosis using STM driven by heterogeneous data fusion. The collected sound and vibration signals of bearings are successively decomposed into multiple frequency band components to extract various time-domain and frequency-domain statistical parameters. A third-order heterogeneous feature tensor is designed based on multi-sensors, frequency band components, and statistical parameters. STM is constructed to preserve the structural information of the third-order heterogeneous feature tensor for bearing fault diagnosis.

The rest of this article is set as follows: Section II introduces the related works and basic principles of STM. The proposed method is described in detail in Section III. Section V is the experimental validation and analysis of the results. Finally, Section VI sums up the whole paper and points out the future plans.

II. RELATED WORKS

A. DATA FUSION STRATEGY

At present, data fusion strategies can be divided into data-level fusion, feature-level fusion, and decision-level fusion. For data-level fusion, Xia *et al.* [23] superimposed the raw time-domain signals from multiple acceleration sensors to form a matrix as the input of the CNN for automatic feature learning and pattern classification. The experiment results verified the superiority of the proposed method over single sensor signals for fault diagnosis experiments of rolling bearings and gearboxes. Akilu *et al.* [24] used cross-power spectral density to fuse the vibration signals from different bearing seats to monitor the operating conditions. Although the data-level fusion method tends to retain as much original information as possible during fusion, the large amount of data leads to high computational complexity, resulting in poor real-time performance of the diagnostic system. Meanwhile, the performance of these data-level fusion methods may not be ideal if simply concatenating signals when they have unidentified formats and sampling rates. In addition, plain concatenation of multi-sensor signals may lead to fuzzy decision boundaries and is difficult to distinguish.

Feature-level fusion refers to firstly extract the respective feature vectors of the multi-source signals and then fuse features to reduce dimensions in a comprehensive manner. Compared with the data-level fusion, feature-level fusion is easier to realize and at the same time can reduce data interference. Feature-level fusion of multi-source signals is also widely used in fault diagnosis. Gangsar *et al.* [25] extracted the multiple statistical features from the vibration signals and current signals of asynchronous motors in different health states and then fused all the statistical features to generate new feature vectors as inputs to the support vector machine (SVM) for state recognition. Shao *et al.* [26] used vibration and voltage signals to construct CNN models based on feature-level fusion for identifying different faults of motors. Jiao *et al.* [27] constructed two parallel coupled dense convolutional networks for automatic feature extraction of vibration signals and speed signals, and then the two types of features are fused for fault classification of planetary gearbox. Qian *et al.* [28] first extracted 40 feature parameters of the vibration signal and three-phase current signals collected from motor and then fused the extracted features into back propagation neural network for distinguishing different fault modes. One of the main challenges of feature-level fusion studies based on multi-source signals is that the performance of the classifier tends to decline as the dimensionality of fused feature vectors increases. In order to overcome this drawback and further improve feature-level fusion effect, researchers have developed various feature dimensionality reduction algorithms.

Decision-level fusion is performed by fusing the results obtained from different diagnosis models trained with multi-source signals. The two main frameworks for decision-level fusion are probability-based fusion and Dempster-Shafer theory. Wang *et al.* [21] proposed a compressor valve fault warning strategy based on multi-source information fusion of vibration, pressure, temperature, and other multi-parameter signals. The experimental results show that the proposed model and warning strategy can effectively realize compressor valve fault warning. Fu *et al.* [29] fused the diagnostic results of induction motors based on vibration signals and current signals at the decision-level fusion of neural networks through dynamic routing algorithm to accomplish the classification of different faults. Wang *et al.* [30] first independently monitored the multi-source sensor signals of rotating machinery using an extended autoregressive model and then fused the results based on the contribution of different sensor signals to achieve state detection of rotating machinery. However, training a series of individual decision models is time-consuming and cumbersome. In addition, in multi-source signal-driven decision-level fusion-driven, the abnormal diagnostic decisions of a few models may seriously interfere with the remaining majority of models, thereby affecting the final fused results.

More importantly, the above-mentioned research cases based on data-level fusion, feature-level fusion, and decision-level fusion are all based on vector space. The vectorization of tensor data may not only generate high-dimensional vectors, leading to increasing computational complexity and overfitting problems, but also lose the structural information of the original tensor data and the coupling information between different monitoring signals, thereby affecting the final intelligent fault diagnosis accuracy.

III. THE PROPOSED METHOD

A. THIRD-ORDER HETEROGENEOUS FEATURE TENSOR DESIGN

Feature extraction is treated as a significant step in intelligent fault diagnosis, usually including time-domain, frequency-domain, and time-frequency-domain techniques. In this paper, in order to simultaneously utilize the available information of multisensors, frequency band components, and statistical parameters, a third-order heterogeneous feature tensor is designed, and the specific process is described as follows.

Firstly, heterogeneous monitoring signals (vibration signals and sound signals) are collected to obtain relatively comprehensive information. To further acquire rich multiscale representations, ensemble empirical mode decomposition is applied to successively decompose the vibration signals and sound signals into multiple frequency band components.

Secondly, various statistical parameters are calculated from each frequency band component of the vibration signals and sound signals, including 10 time-domain and 7 frequency-domain parameters [31].

Finally, a third-order heterogeneous feature tensor is designed, which will not destroy the structural information of multi-source signals. In other words, each sample input into STM can be expressed as a third-order feature tensor, and each order refers to the total number of sensors, frequency band components, and statistical parameters, respectively.

B. STM-BASED INTELLIGENT DIAGNOSIS MODEL CONSTRUCTION

For a tensor sample set $\{\mathrm{X}_i, y_i\}_{i=1}^{l}$, where l is the number of samples and N is the order of $\mathrm{X}_i \in R^{I_1 \times I_2 \times \cdots \cdots \times I_N}$, $y_i \in \{1, -1\}$ is the label of the corresponding tensor sample. For the binary classification problem of tensor space, the proposed STM can transform the classification problem into the following convex quadratic optimization problem.

$$\begin{aligned} &\min_{\mathrm{W},b,\xi} \frac{1}{2}\|\mathrm{W}\|_F^2 + C(1-\theta)\sum_{i=1}^{l_+}\xi_i + C(1+\theta)\sum_{i=1}^{l_-}\xi_i \\ &s.t. \quad y_i(<\mathrm{W},\mathrm{X}> + b) \geq 1 - \xi_i \\ &\xi_i \geq 0, \quad i = 1,2,\ldots,l \end{aligned} \tag{1}$$

$$\theta = \begin{cases} l_+/l & l_+ > l_- \\ 0 & l_+ = l_- \\ -l_-/l & l_+ < l_- \end{cases} \tag{2}$$

where W is the weight tensor of the classification hyperplane, b is the bias, ξ_i is the relaxation variable, C is the penalty factor, l_+ is positive sample, l_- is negative sample, and $<\cdot\,,\cdot>$ is inner product operation. The dynamic parameters θ can be obtained according to the calculation, and it is obvious that when the number of positive and negative tensor samples is equal, that is, the proposed method degenerates into the basic STM.

For solving the optimization problem, the following Lagrange function is constructed:

$$\begin{aligned} L(\mathrm{W},b,\xi_i,\alpha_i,\beta_i) = &\frac{1}{2}\|\mathrm{W}\|_F^2 + C(1-\theta)\sum_{i=1}^{l_+}\xi_i + C(1+\theta)\sum_{i=1}^{l_-}\xi_i \\ &- \sum_{i=1}^{l_+l_-}\beta_i(y_i(<\mathrm{W},\mathrm{X}_i> + b) - 1 + \xi_i) \\ &- \sum_{i=1}^{l_+l_-}\xi_i\alpha_i \end{aligned} \tag{3}$$

where α_i and β_i are Lagrange multipliers.

According to the Kuhn-Tucker condition, the first will take the partial derivative of W, b, and ξ_i, respectively:

$$\frac{\partial L}{\partial \mathrm{W}} = \mathrm{W} - \sum_{i=1}^{l_+ + l_-}\beta_i y_i \mathrm{X}_i \tag{4}$$

$$\frac{\partial L}{\partial b} = -\sum_{i=1}^{l_+ + l_-}\beta_i y_i \tag{5}$$

$$\frac{\partial L}{\partial \xi_i} = C(1-\theta) - \alpha_i - \beta_i, \quad i = 1,2,\ldots,l_+ \tag{6}$$

$$\frac{\partial L}{\partial \xi_i} = C(1+\theta) - \alpha_i - \beta_i, \quad i = 1,2,\ldots,l_- \tag{7}$$

Then, set equations (4)–(7) to zero successively, that is:

$$\mathrm{W} = \sum_{i=1}^{l_+ + l_-}\beta_i y_i \mathrm{X} \tag{8}$$

$$\sum_{i=1}^{l_+ + l_-}\beta_i y_i = 0 \tag{9}$$

$$C(1-\theta) = \alpha_i + \beta_i, \quad i = 1,2,\ldots,l_+ \tag{10}$$

$$C(1+\theta) = \alpha_i + \beta_i, \quad i = 1,2,\ldots,l_- \tag{11}$$

By substituting equations (8)–(11) into optimization problem (3), the corresponding duality problem can be expressed as:

$$\begin{aligned} &\min_{\beta_i} \frac{1}{2}\sum_{i=1}^{l}\sum_{j=1}^{l}\beta_i\beta_j y_i y_j <\mathrm{X}_i,\mathrm{X}_j> - \sum_{i=1}^{n}\beta_i \\ &s.t. \quad \sum_{i=1}^{l}\beta_i y_i = 0 \\ &\quad 0 \leq \beta_i \leq C(1-\theta), \quad i = 1,2,\ldots,l_+ \\ &\quad 0 \leq \beta_i \leq C(1+\theta), \quad i = 1,2,\ldots,l_- \end{aligned} \tag{12}$$

First, for any quantity such as $\mathrm{X}_i \in R^{I_1 \times I_2 \times \cdots \cdots \times I_N}$, the tensor X can first be projected onto Hilbert by the following formula Space.

$$\phi\colon \mathrm{X} \to \phi(\mathrm{X}) \in R^{H_1 \times H_2 \times \cdots \cdots H_P} \tag{13}$$

The above equation can also be called the eigentensor space, where the order of the eigentensor space may not be the same as the order of the eigentensor space, that is, $P \neq N$.

At the same time, the dimensions of each module may also be larger. Thus, the duality problem (12) can be converted to:

$$\min_{\beta_i} \frac{1}{2}\sum_{i=1}^{l}\sum_{j=1}^{l}\beta_i\beta_j y_i y_j < \phi(\mathrm{X}_i),\phi(\mathrm{X}_j) > -\sum_{i=1}^{n}\beta_i$$
$$s.t. \quad \sum_{i=1}^{l}\beta_i y_i = 0 \tag{14}$$
$$0 \le \beta_i \le C(1-\theta), \quad i = 1,2,\ldots,l_+$$
$$0 \le \beta_i \le C(1+\theta), \quad i = 1,2,\ldots,l_-$$

The inner product of its kernel tensor $< \phi(\mathrm{X}_i), \phi(\mathrm{X}_j) >$ can be expressed as $\kappa < \mathrm{X}_i,\mathrm{X}_j >$, which usually selects Gaussian kernel. Directly solving the inner product $< \mathrm{X}_i,\mathrm{X}_j >$ will destroy the intrinsic information of the original tensor. In order to better calculate the inner product $< \mathrm{X}_i,\mathrm{X}_j >$ and retain its intrinsic structure information, Tucker decomposition is introduced to decompose a tensor into a form of a core tensor, and each mode is multiplied by a factor matrix [32].

After solving the above quadratic programming problem to obtain the optimal solution $(\beta_1^*,\beta_2^*,\ldots\ldots,\beta_n^*)^T$, the weight tensor W^* and intercept b^* of the optimal hyperplane can be calculated by the following formulas, respectively.

$$\mathrm{W}^* = \sum_{i=1}^{l}\beta_i^* y_i \phi(\mathrm{X}_i) \tag{15}$$

$$b^* = y_j \sum_{i=1}^{l}\beta_i^* y_i \kappa < \mathrm{X}_i,\mathrm{X}_j > \tag{16}$$

In fact, how to design the feature mapping function is a problem to be further studied. The decision function is expressed as:

$$f(\mathrm{X}) = \mathrm{sgn}\{\sum_{i=1}^{l}\beta_i^* y_i \kappa < \mathrm{X}_i,\mathrm{X} > + b^*\} \tag{17}$$

STM is essentially a multilinear SVM, which can be solved iteratively many times, and the proposed method only needs to be solved once. In addition, STM constructs a hyperplane for each mode in the iterative solution process. For the n-order tensor, STM needs to construct N hyperplanes, while the proposed method only needs to construct one hyperplane. For binary tensor training samples, the computational complexity of STM is $O((l_+ + l_-)^2 NT\prod_{k=1}^{N} I_k)$, where T is the number of cycles, while the computational complexity of the proposed method is $O((l_+ + l_-)^2 R^2 \prod_{k=1}^{N} I_k)$, where R is the tensor factor. It is obvious that the proposed method is significantly superior to the STM model in terms of computational complexity.

In summary, the overall diagnostic flow of the proposed method can be shown in Fig. 1.

IV. EXPERIMENTS

A. INTRODUCTION TO EXPERIMENT PLATFORM AND HETEROGENEOUS MONITORING DATA

Bearing as a key component in rotating machinery, its health state directly affects the operation of the entire equipment. The experimental platform for bearing fault simulation and heterogeneous data collection is shown in Fig. 2, mainly consisting of an induction motor, two bearing housings, a rotor system, a vertical vibration sensor (contact measurement), a horizontal vibration sensor (contact measurement), and a sound sensor (non-contact measurement). The data acquisition system is LMS, and the heterogeneous signals are collected under the rotational speed of 1500 rpm with sampling frequency of 25.6 kHz.

Three types of fault modes of bearings are created, including outer ring fault (OF), inner ring fault (IF), and roller fault (RF). Each fault condition has three different sizes of damage, that are 0.2, 0.4, and 0.6 mm, respectively. Therefore, a total of ten health conditions are constructed, defined as normal condition (Label 1), inner race fault with 0.2 mm (IF1, Label 2), inner race fault with 0.4 mm (IF2, Label 3), inner race fault with 0.6 mm (IF3, Label 4), roller fault with 0.2 mm (RF1, Label 5), roller fault with 0.4 mm (RF2, Label 6), roller fault with 0.6 mm (RF3, Label 7), outer race fault with 0.2 mm (OF1, Label 8), outer race fault with 0.4 mm (OF2, Label 9), and outer race fault with 0.6 mm (OF3, Label 10).

Take the damage size of 0.2 mm as example, the pictures of three faulty bearings are illustrated in Fig. 3. The original time-domain vertical vibration signals and sound signals of the nine fault states of bearings are given in Fig. 4 (1024 point as example), where the horizontal coordinate indicates the sampling data points, and the vertical coordinate indicates the amplitude ($\mathrm{m/s^2}$).

B. COMPARISON EXPERIMENTS AND EVALUATION INDICATORS

In this paper, the proposed method is applied to class-imbalanced fault diagnosis with the help of heterogeneous information fusion. To verify the diagnostic performance of the proposed method, SVM, least square support vector machine (LSSVM), and maximum margin classifier with flexible convex hulls (MMC_FCH) were selected as comparative analysis methods in analyzing the same imbalanced datasets. Some samples from each health state were randomly selected as the training data, and the remaining samples from each state were used for testing.

Six groups of experiments with different imbalanced ratios, data fusion ways, and classification scenarios are designed, and the detailed dataset descriptions are listed in Table I (10 classification tasks), Table II (7 classification tasks), and Table III (4 classification tasks). It should be noticed that Experiments 5 and 6 apply this method not only to the class unbalanced fault diagnosis based on heterogeneous information fusion but also to the class unbalanced fault diagnosis based on the fusion of vertical and horizontal vibration signals.

In order to quantitatively evaluate the classification performance of the proposed method and the comparison methods, precision (Pr), recall (Re), F-score, and Geometric Mean (G-mean) are selected as the indicators, with the corresponding formulas.

$$\mathrm{Re} = \frac{TP}{TP + FN} \tag{18}$$

$$\mathrm{Pr} = \frac{TP}{TP + FP} \tag{19}$$

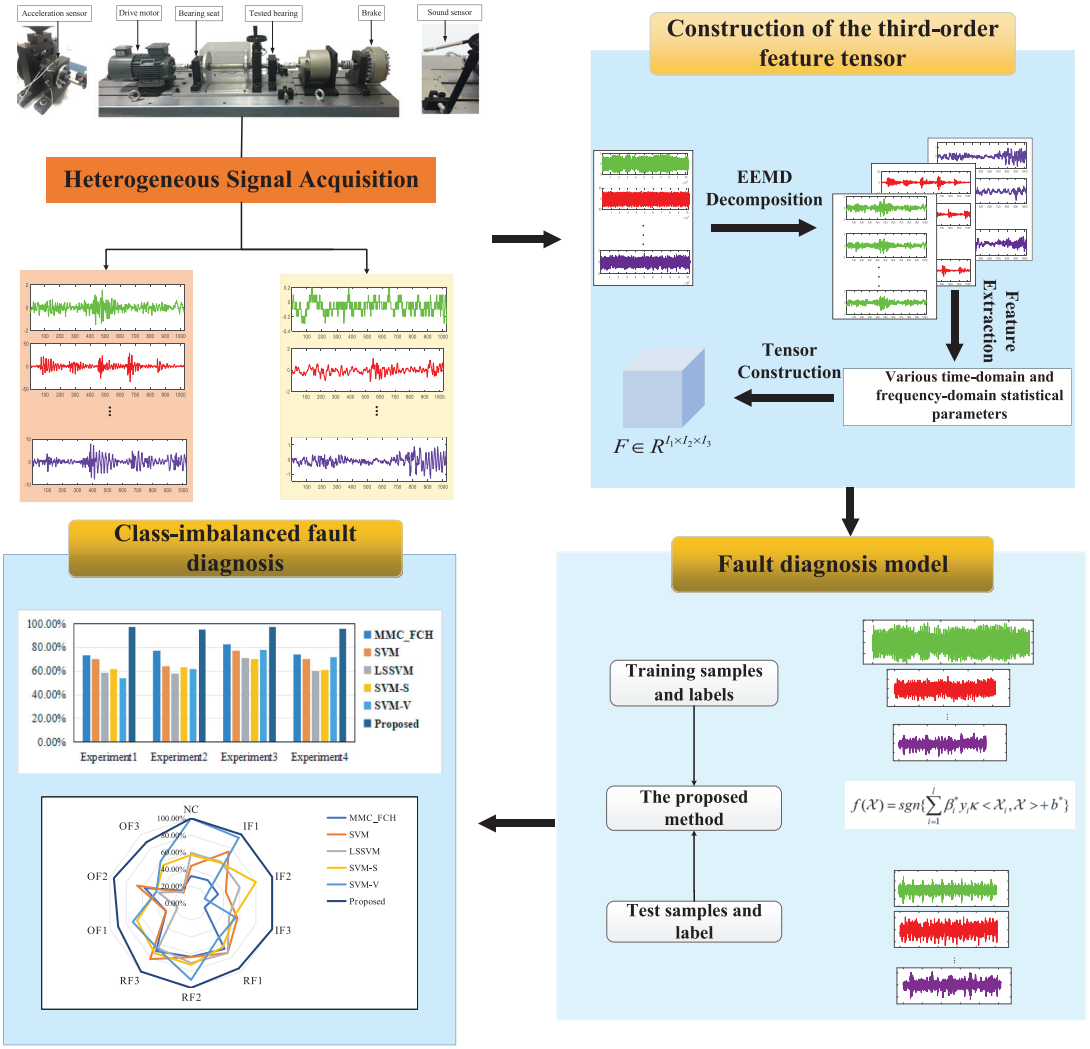

Fig. 1. The overall diagnostic flow of the proposed method.

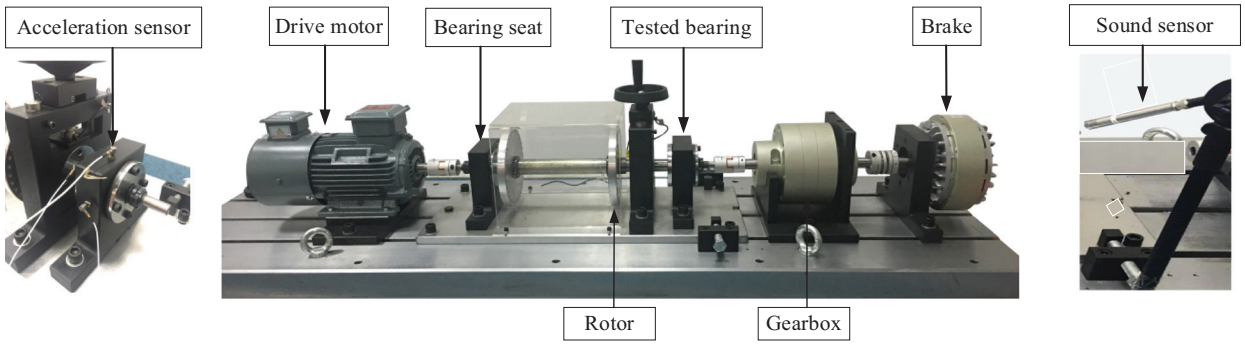

Fig. 2. Experimental platform for bearing fault simulation and heterogeneous data collection.

$$\text{F-score} = \frac{2 \times \text{Pr} \times \text{Re}}{\text{Pr} + \text{Re}} \tag{20}$$

$$\text{G-mean} = \sqrt{\text{Pr} \times \text{Re}} \tag{21}$$

where TP is the number of positive samples that are correctly classified as positive, FN is the number of positive samples incorrectly classified as negative, and FP is the number of negative samples incorrectly classified as positive.

C. COMPARATIVE ANALYSIS OF RESULTS

In Experiments 1–6, each method is repeated 10 times to ensure the stability and reliability of the results. The average values of the above four indicators after these 10 trials are used as the final results for the overall diagnosis, as listed in

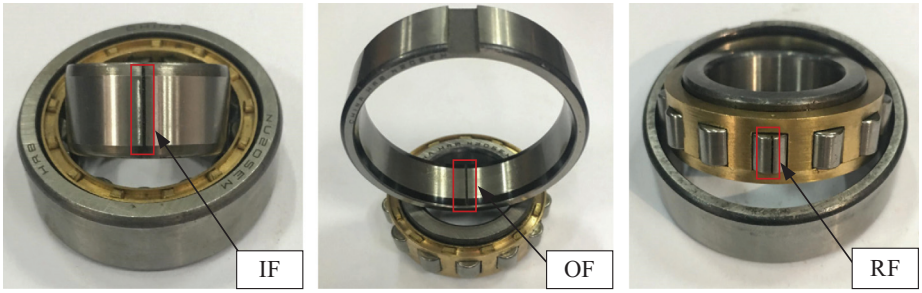

Fig. 3. Three faulty bearings with 0.2 mm damage size.

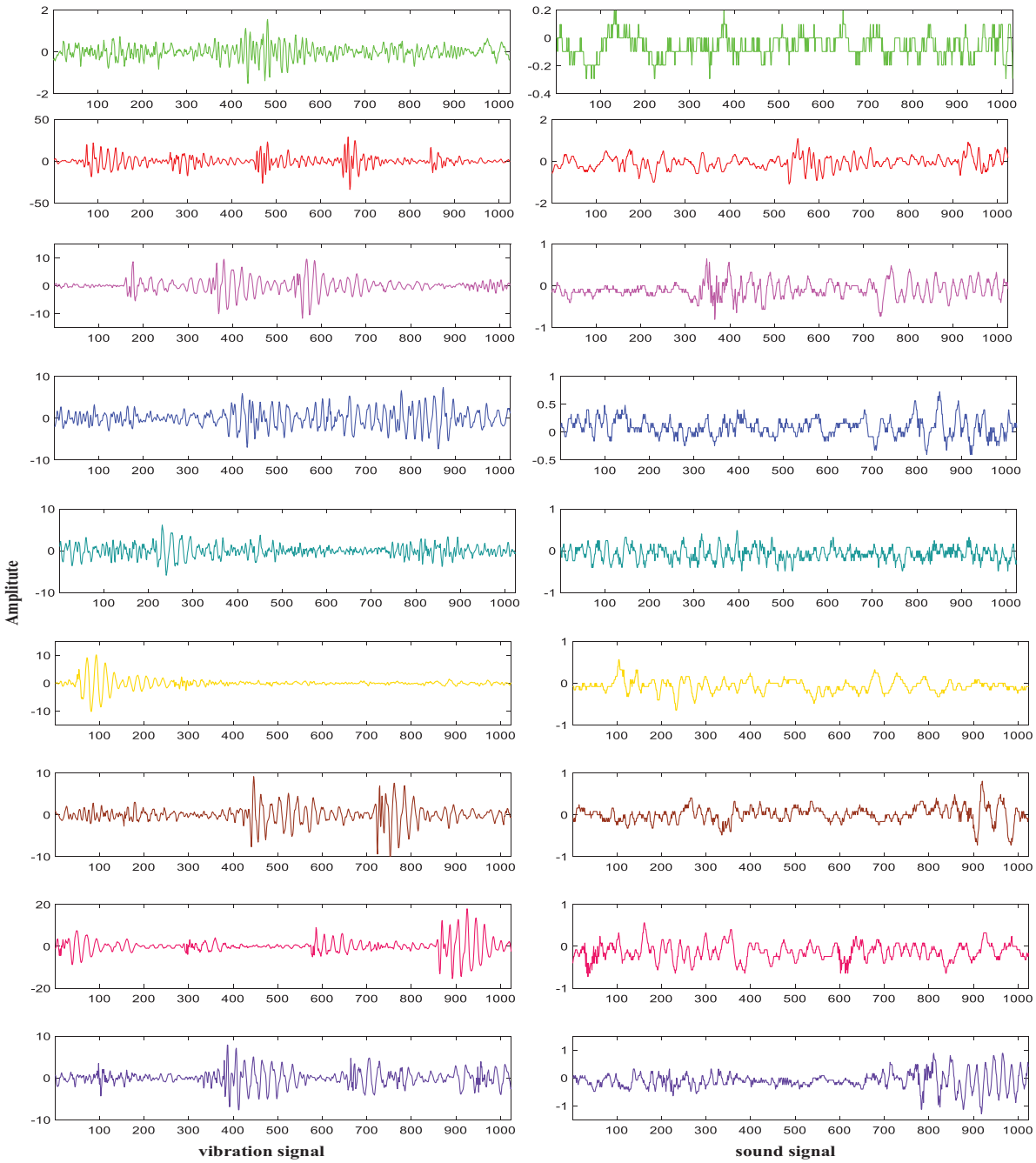

Fig. 4. Original signal waveforms of nine faulty conditions.

Table I. Detailed dataset description for Experiment 1 and Experiment 2

Experiment 1		Experiment 2	
Health states	Numbers of training/testing samples	Health states	Numbers of training/testing samples
NC	90/10	NC	80/10
IF1	20/10	IF1	20/10
IF2	20/10	IF2	20/10
IF3	20/10	IF3	20/10
RF1	30/10	RF1	20/10
RF2	30/10	RF2	20/10
RF3	30/10	RF3	20/10
OF1	15/10	OF1	15/10
OF2	15/10	OF2	15/10
OF3	15/10	OF3	15/10

Table II. Detailed dataset description for Experiment 3 and Experiment 4

Experiment 3		Experiment 4	
Health states	Numbers of training/testing samples	Health states	Numbers of training/testing samples
NC	90/10	NC	80/10
IF1	20/10	IF1	20/10
IF2	20/10	IF2	20/10
RF1	30/10	RF1	20/10
RF2	30/10	RF2	20/10
OF1	15/10	OF1	15/10
OF2	15/10	OF2	15/10

Tables IV–VII. The input data of SVM-S is a single sound signal, and the input data of SVM-V is a single vertical vibration signal. The inputs of other comparison methods are all in vector form using the concatenation of vibration signal and sound signal. The hyperparameters of all the methods are determined using cross-validation methods. In

Table III. Detailed dataset description for Experiment 5 and Experiment 6

Experiment 5		Experiment 6	
Health states	Numbers of training/testing samples	Health states	Numbers of training/testing samples
NC	210/10	NC	200/20
IF1	15/10	IF1	20/20
RF1	15/10	IF2	20/20
OF1	15/10	IF3	20/20

Experiment 5 and Experiment 6, the input data of SVM-VxVy is the vector of vertical and horizontal vibration signals, and the input data of SVM-SV is the vector of vertical vibration signal and sound signal. The input data of MMC_FCH-VxVy is the splicing vector of vertical and horizontal vibration signals, and the input data of MMC_FCH-SV is the splicing vector of vertical vibration signal and sound signal. The input data of LSSVM-VxVy is the spliced vector of vertical and horizontal vibration signals, and the input data of LSSVM-SV is the spliced vector of vertical vibration signal and sound signal.

From the classification results shown in Tables IV and V, it can be seen that in these four experiments, the proposed method has achieved better classification results in terms of both precision rate and recall rate compared with other methods. Specifically, the precision rates of the proposed method in Experiments 1–4 are 96.0%, 93.0%, 96.0%, and 96.5%, respectively. The recall rates of the proposed method in Experiments 1–4 are 97.0%, 94.0%, 97.0%, and 96.0%, respectively. In addition, it can be clearly seen from Tables IV and V that the classification effects of tensor classifiers are significantly better than vector classifiers.

It can be seen from the classification results in Table VI that the method proposed in Experiment 5 has achieved better performance in class-imbalanced fault diagnosis tasks than other methods in terms of precision rate, recall rate, F-score, and G-mean. The precision of the proposed method is 98.0% in the classification of heterogeneous tensor and 97.0% in the classification of vertical vibration signal tensor. The recall rate of the proposed method is 97.0% in the classification of heterogeneous tensors, and

Table IV. Precision rate of different methods in class-imbalanced bearing fault diagnosis

Experiments	MMC_FCH	SVM	LSSVM	SVM-S	SVM-V	Proposed
Experiment 1	73.0%	70.0%	59.0%	62.0%	54.0%	96.0%
Experiment 2	77.0%	64.0%	58.0%	63.0%	62.0%	93.0%
Experiment 3	83.0%	77.0%	71.0%	70.0%	78.0%	96.0%
Experiment 4	74.0%	70.0%	60.0%	61.0%	72.0%	96.5%

Table V. Recall rate of different methods in class-imbalanced bearing fault diagnosis

Experiments	MMC_FCH	SVM	LSSVM	SVM-S	SVM-V	Proposed
Experiment 1	43.0%	56.0%	60.0%	63.0%	68.0%	97.0%
Experiment 2	45.0%	51.0%	45.0%	56.0%	64.0%	94.0%
Experiment 3	61.0%	59.0%	63.0%	64.0%	80.0%	97.0%
Experiment 4	41.0%	61.0%	56.0%	60.0%	73.0%	96.0%

Table VI. Classification results of each model in Experiment 5

Methods	Precision	Recall	F-score	G-mean
SVM-V	93.50%	93.25%	93.38%	93.33%
SVM-S	77.00%	59.00%	66.80%	67.40%
SVM-VxVy	73.50%	68.50%	70.90%	71.00%
SVM-SV	75.50%	70.50%	72.90%	72.95%
MMC_FCH-VxVy	92.67%	92.33%	92.50%	92.50%
MMC_FCH-SV	87.00%	86.00%	86.50%	86.50%
LSSVM-VxVy	84.00%	83.50%	83.50%	83.50%
LSSVM-SV	82.50%	76.75%	79.50%	79.58%
Proposed-VxVy	97.00%	96.00%	96.50%	96.50%
Proposed-SV	98.00%	97.00%	97.50%	97.50%

Table VII. Classification results of each model in Experiment 6

Methods	Precision	Recall	F-score	G-mean
SVM-V	90.75%	88.50%	89.63%	89.63%
SVM-S	86.00%	80.00%	82.90%	82.90%
SVM-VxVy	67.50%	63.50%	65.45%	65.50%
SVM-SV	73.00%	67.50%	70.10%	70.20%
MMC_FCH-VxVy	91.00%	90.00%	90.50%	90.50%
MMC_FCH-SV	88.33%	86.00%	87.17%	87.17%
LSSVM-VxVy	87.00%	86.00%	86.50%	86.50%
LSSVM-SV	79.75%	75.75%	77.70%	77.73%
Proposed-VxVy	97.00%	96.25%	96.63%	96.63%
Proposed-SV	99.00%	98.80%	99.00%	98.80%

96.0% in the classification of vertical vibration signal tensor. The F-score of the proposed method is 97.5% for the classification of heterogeneous tensors and 96.5% in the classification of vertical vibration signal tensor. The G-mean of this method is 97.5% for the classification of heterogeneous tensors and 96.5% in the classification of vertical vibration signal tensor. Similarly, according to the results in Table VII, the method proposed in Experiment 6 has achieved better results than other methods in terms of the four indicators.

In order to further explore the detailed diagnostic results of the proposed method, the statistical graphs of G-mean and F-score values are given, as shown in Figs. 5 and 6. It can be seen from Figs. 5 and 6 that specifically, the F-score values of the proposed method in Experiments 1-4 are 97.0%, 94.5%, 97.0%, and 96.0%, respectively, which is more than SVM-V (69.5%, 63%, 79%, 72.5%), SVM-S (65.4%, 59.3%, 66.9%, 60.5%), LSSVM (59.5%, 50.7%, 66.8%, 58%), SVM (62.2%, 56.8%, 66.8%, 65.2%), and MMC_FCH (54.1%, 56.8%, 70.3%, 52.8%). There is also a highly similar phenomenon in G-mean values.

These results further confirm that the diagnostic performance of the proposed method driven by heterogeneous data fusion is significantly better than the vector classifiers in class-imbalanced machinery fault diagnosis. However, the vectorization of multi-source signal features using simple concatenation may not be conducive to improving diagnostic accuracy due to the fact that high-dimensional vectors usually lead to high complexity and overfitting problems. Besides, it seems that single vibration signal is better than single sound signal for fault diagnosis using SVM and other vector classifiers.

Furthermore, to investigate the diagnostic effect of each model on each type of fault, the G-mean radar chart and F-score radar chart of each type are specially given, as shown in Figs. 7 and 8, respectively. It can be seen that

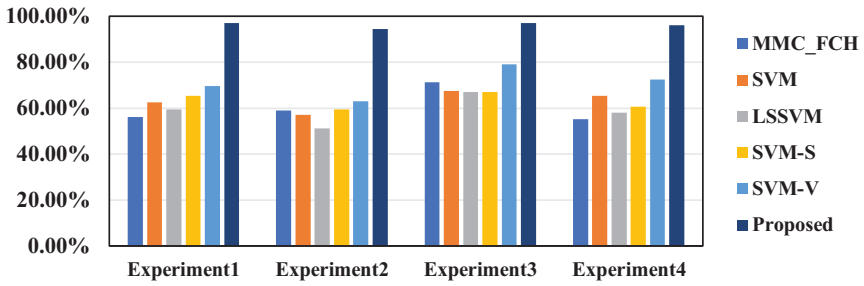

Fig. 5. F-score values of each method in four class-imbalanced fault diagnosis experiments.

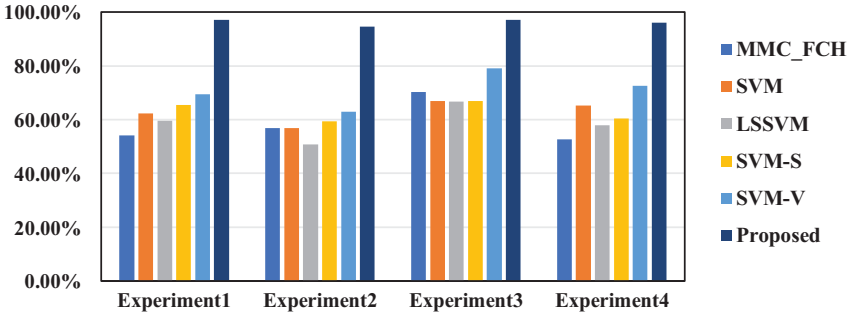

Fig. 6. G-mean values of each method in four class-imbalanced fault diagnosis experiments.

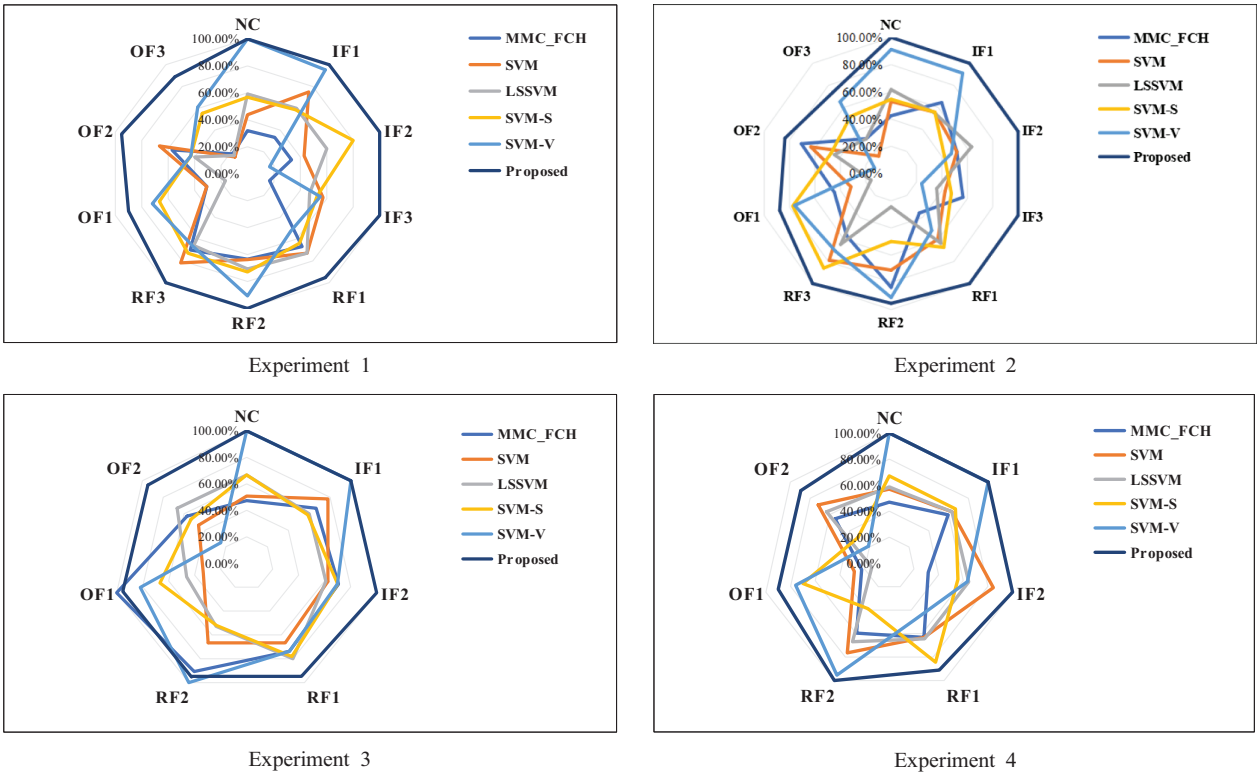

Fig. 7. F-score values of each condition using different methods in four class-imbalanced fault diagnosis.

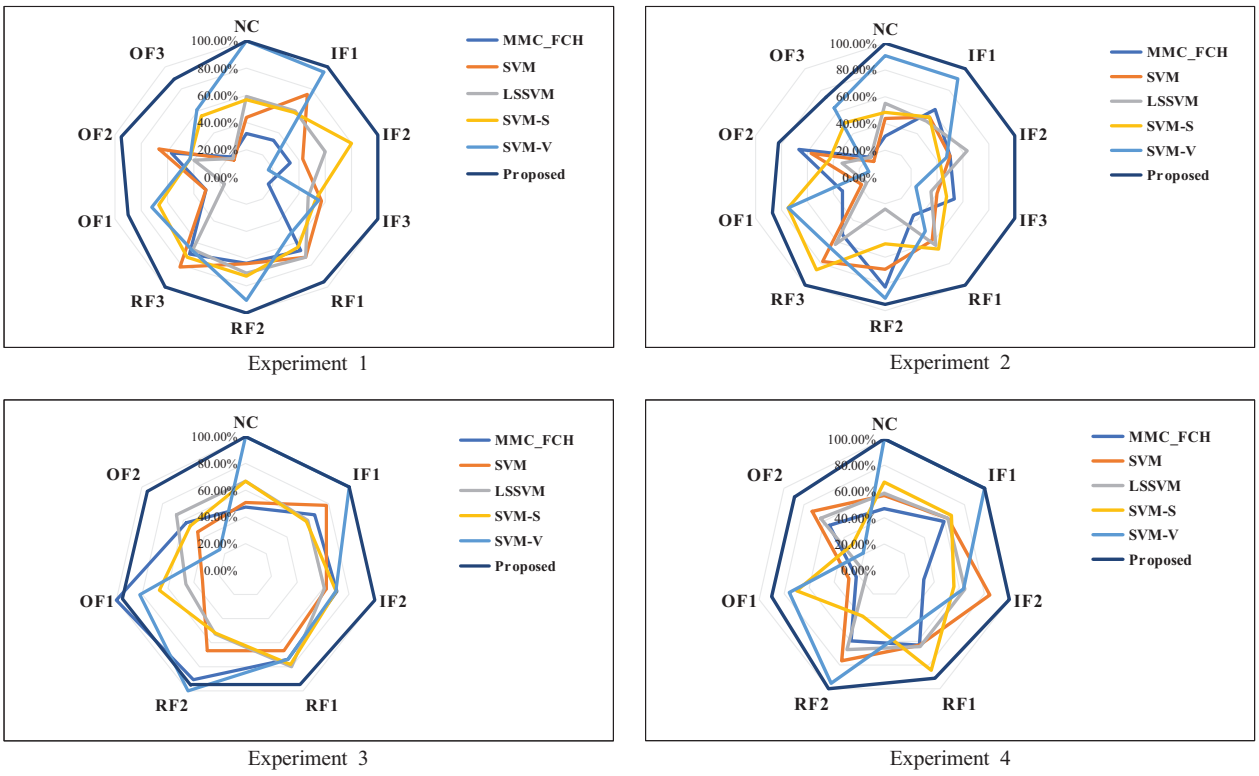

Fig. 8. G-mean values of each condition using different methods in four class-imbalanced fault diagnosis.

SVM shows relatively unsatisfactory fault classification effect for each category using sound signals. With the help of vibration signals, SVM is less effective than other fault types in classifying outer ring fault with 0.4 mm. Similar to SVM, the other vector classifiers are also not ideal. Besides, it can be found that the proposed method can

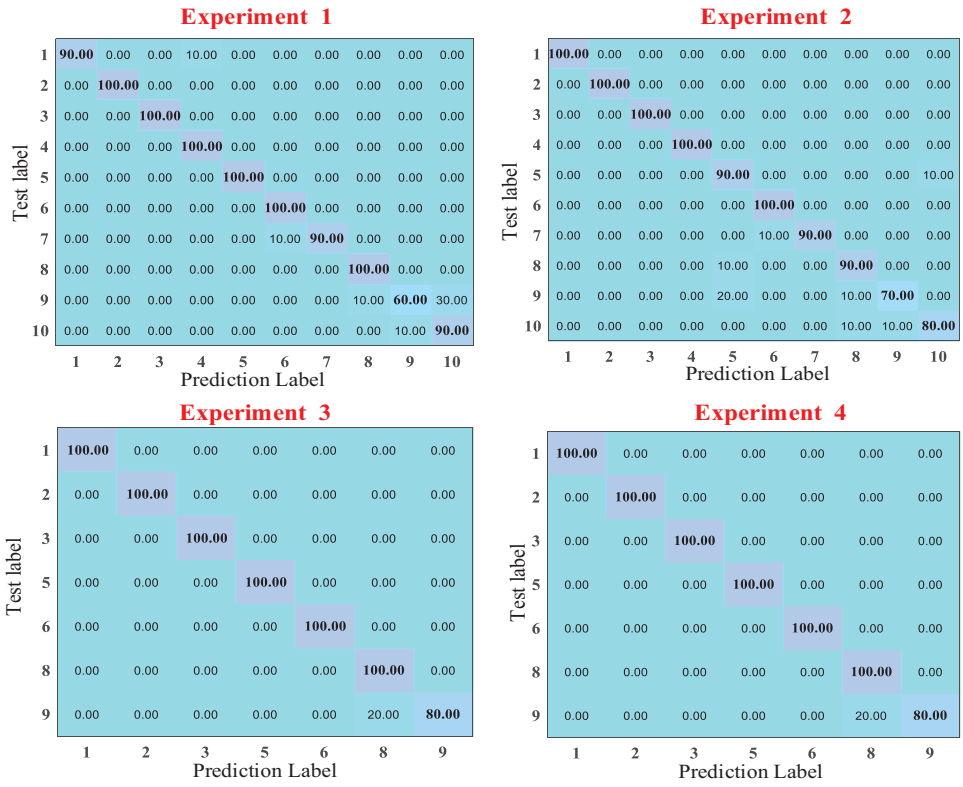

Fig. 9. Confusion matrixes of the proposed method in four class-imbalanced fault diagnosis.

achieve the best results in the diagnosis of various fault categories in the four experiments. Figure 9 shows the confusion matrixes of the proposed method in four class-imbalanced fault diagnosis, which clearly records all the misclassification information in detail. In Fig. 9, the horizontal and vertical axes refer to the prediction labels and true labels (test labels), respectively. The accuracy for each individual state can be found from diagonal elements, and the elements at other places of confusion matrixes refer to the misclassification rates.

V. CONCLUSIONS

Aiming to fully preserve the structural information of heterogeneous signals to improve diagnostic accuracy and stability in class-imbalanced fault diagnosis tasks, this paper proposes a new method based on STM and heterogeneous data fusion. In this method, firstly, the collected sound and vibration signals of bearings are successively decomposed into multiple frequency band components to extract various time-domain and frequency-domain statistical parameters. Then, according to multisensors, frequency band components, and statistical parameters, a third-order heterogeneous feature tensor is designed. Finally, an intelligent diagnosis model based on STM is constructed to preserve the structural information of the third-order heterogeneous feature tensor for bearing fault diagnosis.

A series of comparative experiments with different imbalanced ratios, data fusion ways, and classification scenarios are designed to verify the advantages of the proposed method. The results confirm that the proposed method has achieved better performance in class-imbalanced fault diagnosis tasks than other methods in terms of precision rate, recall rate, F-score, and G-mean. Heterogeneous data fusion-driven class-imbalanced fault diagnosis of machinery has broad research space, and we will continue to study.

ACKNOWLEDGEMENTS

This research is supported by the National Natural Science Foundation of China (No. 52275104), and the Science and Technology Innovation Program of Hunan Province (No. 2023RC3097).

CONFLICT OF INTEREST STATEMENT

The authors declare no conflicts of interest.

REFERENCES

[1] Z. Cao, J. Dai, W. Xu, and C. Chang, "Sparse Bayesian learning approach for compound bearing fault diagnosis," *IEEE Trans. Ind. Inf.*, vol. 20, no. 2, pp. 1562–1574, 2024.

[2] R. Rajabioun, M. Afshar, M. Mete, Ö. Atan, and B. Akin, "Distributed bearing fault classification of induction motors using 2-D deep learning model," *IEEE J. Emerging Sel. Topics Ind. Electronics*, vol. 5, no. 1, pp. 115–125, 2024.

[3] M. R. Barusu and M. Deivasigamani, "Non-Invasive vibration measurement for diagnosis of bearing faults in 3-phase squirrel cage induction motor using microwave sensor," *IEEE Sens. J.*, vol. 21, no. 2, pp. 1026–1039, 2021.

[4] Y. Zhang and J. Ji, "Intelligent fault diagnosis of a reciprocating compressor using mode isolation convolutional deep

belief networks," *IEEE/ASME Trans. Mechatron.*, vol. 26, no. 3, pp. 1668–1677, 2021.

[5] S. Xing, Y. Lei, S. Wang, and F. Jia, "Distribution-invariant deep belief network for intelligent fault diagnosis of machines under new working conditions," *IEEE Trans. Ind. Electron.*, vol. 68, no. 3, pp. 2617–2625, 2021.

[6] N. Qin, K. Liang, D. Huang, L. Ma, and A. H. Kemp, "Multiple convolutional recurrent neural networks for fault identification and performance degradation evaluation of high-speed train bogie," *IEEE Trans. Neural Netw. Learn. Syst.*, vol. 31, no. 12, pp. 5363–5376, 2020.

[7] A. Zollanvari, K. Kunanbayev, S. Akhavan Bitaghsir, and M. Bagheri, "Transformer fault prognosis using deep recurrent neural network over vibration signals," *IEEE Trans. Instrum. Meas.*, vol. 70, p. 2502011, 2021.

[8] S. Turizo, G. Ramos, and D. Celeita, "Voltage sags characterization using fault analysis and deep convolutional neural networks," *IEEE Trans. Ind. Appl.*, vol. 58, no. 3, pp. 3333–3341, 2022.

[9] D. Chen, R. Liu, Q. Hu, and S. X. Ding, "Interaction-aware graph neural networks for fault diagnosis of complex industrial processes," *IEEE Trans. Neural Netw. Learn. Syst.*, vol. 34, no. 9, pp. 6015–6028, 2023.

[10] H. Shao, M. Xia, G. Han, Y. Zhang, and J. Wan, "Intelligent fault diagnosis of rotor-bearing system under varying working conditions with modified transfer convolutional neural network and thermal images," *IEEE Trans. Ind. Inf.*, vol. 17, no. 5, pp. 3488–3496, 2021.

[11] Y. Su, L. Meng, X. Kong, T. Xu, X. Lan, and Y. Li, "Generative adversarial networks for gearbox of wind turbine with unbalanced data sets in fault diagnosis," *IEEE Sens. J.*, vol. 22, no. 13, pp. 13285–13298, 2022.

[12] D. Dablain, B. Krawczyk, and N. V. Chawla, "Deep SMOTE: fusing deep learning and SMOTE for imbalanced data," *IEEE Trans. Neural Netw. Learn. Syst.*, vol. 34, no. 9, pp. 6390–6404, 2023.

[13] Z. Li et al., "A novel method for imbalanced fault diagnosis of rotating machinery based on generative adversarial networks," *IEEE Trans. Instrum. Meas.*, vol. 70, p. 3500417, 2020.

[14] Y. Chen, Z. Hong, and X. Yang, "Cost-sensitive online adaptive kernel learning for large-scale imbalanced classification," *IEEE Trans. Knowl. Data Eng.*, vol. 35, no. 10, pp. 10554–10568, 2023.

[15] Q. He, Y. Pang, and G. Jiang. "A Spatio-temporal multiscale neural network approach for wind turbine fault diagnosis with imbalanced SCADA data," *IEEE Trans. Ind. Inf.*, vol. 17, no. 10, pp. 6875–6884, 2021.

[16] S. Han, H. Shao, Z. Huo, X. Yang, and J. Cheng. "End-to-end chiller fault diagnosis using fused attention mechanism and dynamic cross-entropy under imbalanced datasets," *Build. Environ.*, vol. 212, p. 108821, 2022.

[17] D. Ruan et al., "Collaborative optimization of CNN and GAN for bearing fault diagnosis under unbalanced datasets," *Lubr.*, vol. 9, no. 10, p. 105, 2021.

[18] Z. He, H. Shao, J. Cheng, X. Zhao, and Y. Yang, "Support tensor machine with dynamic penalty factors and its application to the fault diagnosis of rotating machinery with unbalanced data," *Mech. Syst. Sig. Process.*, vol. 141, p. 106441, 2020.

[19] C. Hu, S. He, and Y. Wang. "A classification method to detect faults in a rotating machinery based on kernelled support tensor machine and multilinear principal component analysis," *Appl. Intelligence*, vol. 51, no. 4, pp. 2609–2621, 2021.

[20] C. Yang and M. Jia. "Hierarchical multiscale permutation entropy-based feature extraction and fuzzy support tensor machine with pinball loss for bearing fault identification," *Mech. Syst. Sig. Process.*, vol. 149, p. 107182, 2021.

[21] Wang H et al., "Early warning of reciprocating compressor valve fault based on deep learning network and multi-source information fusion," *Trans. Inst. Meas. Control*, vol. 45, no. 4, pp. 777–789, 2022.

[22] H. Shao, J. Lin, L. Zhang, D. Galar, and U. Kumar, "A novel approach of multisensory fusion to collaborative fault diagnosis in maintenance," *Inf. Fusion*, vol. 74, pp. 65–76, 2021.

[23] M. Xia et al., "Fault diagnosis for rotating machinery using multiple sensors and convolutional neural networks," *IEEE/ASME Trans. Mechatron.*, vol. 231, no. 1, pp.101–110, 2018.

[24] Y. K. Akil, J. K. Sinha, and K. Elbhbah. "An improved data fusion technique for faults diagnosis in rotating machines," *Measurement*, vol. 58, pp. 27–32, 2014.

[25] P. Gangsar et al., "Diagnostics of combined mechanical and electrical faults of an electromechanical system for steady and ramp-up speeds," *J. Vib. Eng. Technol.*, vol. 10, no. 4, pp.1431–1450, 2022.

[26] S. Shao et al., "DCNN-based multi-signal induction motor fault diagnosis," *IEEE Trans. Instrum. Meas.*, vol. 69, no. 6, pp.2658–2669, 2020.

[27] J. Jiao et al., "Deep coupled dense convolutional network with complementary data for intelligent fault diagnosis," *IEEE Trans. Ind. Electron.*, vol. 66, no. 12, pp. 9858–9867, 2019.

[28] G. Qian et al., "Edge computing: a promising framework for real-time fault diagnosis and dynamic control of rotating machines using multi-sensor data," *IEEE Sens. J.*, vol. 19, no. 11, pp. 4211–4220, 2019.

[29] P. Fu et al., "Dynamic routing-based multimodal neural network for multi-sensory fault diagnosis of induction motor," *J. Manuf. Syst.*, vol. 55, pp. 264–272, 2020.

[30] T. Wang, G. Lu, and P. Yan. "Multi-sensors based condition monitoring of rotary machines: an approach of multidimensional time-series analysis," *Measurement*, vol. 134, pp. 326–335, 2019.

[31] X. Yan and M. Jia, "A novel optimized SVM classification algorithm with multi-domain feature and its application to fault diagnosis of rolling bearing," *Neurocomputing*, vol. 313, pp. 47–64, 2018.

[32] J. G. Jang, M. Park, J. Lee, and L. Sael, "Large-scale tucker Tensor factorization for sparse and accurate decomposition," *J. Supercomput.*, vol. 78, no. 16, pp.17992–18022, 2022.